Highly Tunable Heterodyne Sub-THz Wireless Link Entirely Based on Optoelectronics

Highly Tunable Heterodyne Sub-THz Wireless Link Entirely Based on Optoelectronics

Alvaro Morales, *Student Member, IEEE,* Gleb Nazarikov, Simon Rommel, *Member, IEEE,* Chigo Okonkwo, *Senior Member, IEEE,* and Idelfonso Tafur Monroy, *Senior Member, IEEE*

***Abstract*—This article presents the experimental demonstration of a fully photonics-based heterodyne sub-THz system for wireless communications. A p-i-n photodiode is used as a broadband transmitter to up-convert the signal to the sub-THz domain and a photoconductive antenna down-converts the received wave to an intermediate frequency around 3.7 GHz. The optical signals used for photomixing are extracted from two independent optical frequency combs with different repetition rates. The optical phase locking reduces the phase noise of the sub-THz signal, greatly improving the performance of the system when phase modulation formats are transmitted. The sub-THz carrier is tuned between 80 GHz and 320 GHz in 40 GHz steps, showing a power variation of 21.8 dB. The phase noise at both ends of the communication link is analyzed and compared with the phase noise of the received signal with different wireless carriers. As a proof-of-concept, a 100 Mbit/s BPSK signal is successfully transmitted over 80 GHz, 120 GHz, and 160 GHz carriers, achieving a bit error rate below 10^{-5} in the first two cases. These results show the great potential of THz communications driven by photonics to cover an extensive portion of the THz range without relying on electronic components that limit the operating range of the system to a concrete frequency band.**

***Index Terms*—Sub-THz communications, THz heterodyne detection, photomixing, optical frequency comb, phase noise.**

I. Introduction

THE ever-increasing demand for higher data rates in wireless communications inevitably leads to the exploration of new frequency allocations in the sub-terahertz (sub-THz) and terahertz (THz) bands [1]–[3]. Although the THz frequency range is in general defined as the gap between microwaves and infrared waves (0.3 – 10 THz), only some windows in the lower region and below (0.1 – 1 THz) are suitable for wireless communications due to the high attenuation or strong atmospheric absorption elsewhere. The available spectral resources in this range of the electromagnetic spectrum promise to fulfill the capacity demands of future communication standards, reaching data rates of 100 Gbit/s and beyond [1]. This trend drives the development of more efficient THz systems and components operating at room temperature, aiming to cover a transmission bandwidth of hundreds of gigahertz, supporting broadband modulation formats and increasing the transmission distance.

Manuscript received April 22, 2020; revised December 11, 2020. This work was partly funded by the H2020 ITN CELTA and H2020 blueSPACE projects under grant Nos. 675683 and 762055 as well as the NWO HTSM project FREEPOWER under project No. 17094.

A. Morales, G. Nazarikov, S. Rommel, C. Okonkwo and I. Tafur Monroy are with the Department of Electrical Engineering, Eindhoven University of Technology, 5600 MB Eindhoven, the Netherlands, (e-mail: a.morales.vicente@tue.nl).

Different technologies and methods are used to generate and detect sub-THz and THz waves in many applications [4]. The main approaches that are suitable for wireless communications can be classified into two categories: electronics and optoelectronics. The signal power in electronic systems is typically better than that of their purely optoelectronic counterparts, which require hybrid solutions based on electronic amplifiers to overcome their power limitations [1]. However, the operating range for the frequency in electronic devices is, in general, lower as many of them are limited to a concrete frequency band. This category includes low-frequency signal generators followed by a chain of multipliers, sub-harmonic mixers and resonant tunneling diodes (RTD) among others [5]–[7]. As electronic receivers, waveguide envelope detectors and mixers can be used depending on the modulation format [8]. Furthermore, many breakthroughs have been achieved in THz power amplifiers and low noise amplifiers [9], [10]. The optoelectronic approaches for signal generation are based on the heterodyning of two optical signals – de-tuned by the intended wireless carrier frequency – on a high bandwidth photodiode. Both p-i-n and uni-travelling carrier (UTC) photodiodes have been used for this purpose [11], [12]. The main advantage of this solution is the possibility to cover a large portion of the THz range by simply tuning the frequency difference between two optical carriers and the ability to multiplex different channels in frequency [13]. Similarly, photoconductors can be used to detect THz waves. Although this technique is not common for communications, it has been widely used in other applications like spectroscopy [14].

Although electronic components (e.g., power amplifiers) are required to face the high attenuation of wireless propagation at sub-THz and THz frequencies [15] (see Fig. 1), they prevent systems from fully exploiting the available spectral resources. Moreover, using the same technology for signal transmission and detection will facilitate the implementation of bidirectional links, as will be required in real deployments [16]. Future THz communications will therefore rely on photonics to implement ultra-broadband, highly tunable, multi-channel, and bidirectional links, potentially achieving channel allocations of several gigahertz over a tuning range of hundreds of gigahertz. This scenario is not yet possible, especially for transmission distances higher than several meters, because of the limited dynamic range. The transmission attenuation is in the order of 100 dB for distances longer than 2 m as can be observed in Fig. 1. A possible solution to increase the transmitted power is to use phased antenna arrays, offering extra functionalities like beamforming [17]. Nevertheless, ultra-broadband short-range

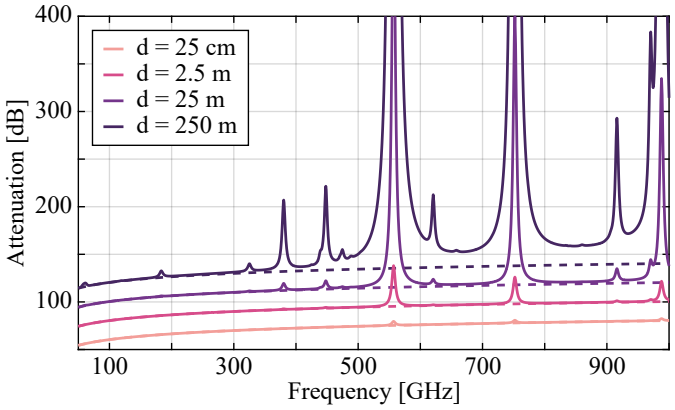

Fig. 1. Attenuation in a wireless link due only to free space propagation (dashed lines) and including atmospheric absorption (solid lines) for different transmission distances, d. The graphs were calculated assuming 7.5 g/m^3 water vapor density and 15 °C temperature according to [15].

wireless links (< 1 m) also have many applications such as personal area networks (PAN), kiosk downloading and inter-rack wireless communications in data centers [18].

Some works have already attempted to establish heterodyne wireless links driven by optoelectronic techniques, covering a wide range in the sub-THz domain [19]. The first realizations of communication links using optoelectronics at both sides have been recently reported [20], [21]. In these works, multi-channel transmissions in the 300-GHz band were successfully demonstrated, achieving an aggregated bit rate of 30 Gb/s and a wireless distance of 58 m [21]. Waveguided horn antennas and power amplifiers were employed to achieve these figures, limiting the operating range to the waveguide frequency band. A transmission in the 100-GHz range without THz amplifiers and a wireless distance of 7 cm is also included, with some modifications in the system [21]. Another essential aspect to take into consideration when a THz signal is generated/detected by photomixing is the phase noise. When two independent laser sources are used, the phase distortions of both contribute to the instability of the resulting THz signal. This fact will degrade the signal quality when phase modulation is used, impeding advanced phase modulation formats or imposing heavy equalization requirements. This can be solved using two phase-locked signals, for example, extracted from an optical frequency comb (OFC).

The practical realization of a broadband wireless link, with enough flexibility to sweep the wireless carrier over a wide range without frequency-limiting electronics, using phase-locked optical signals to generate stable signals, is still an open challenge to be addressed. In this paper, we experimentally demonstrate a heterodyne sub-THz wireless link entirely based on optoelectronic techniques. Optical signals extracted from two independent OFCs, generated by a phase modulator and a pico-second laser, are used to drive a THz photodiode serving as emitter, and a photoconductive antenna (PCA) used as receiver. A continuous wave (CW) signal from 80 GHz to 320 GHz in 40 GHz steps is down-converted to an intermediate frequency around 3.7 GHz. A 100 Mbit/s BPSK is successfully transmitted at 80 GHz, 120 GHz and 160 GHz wireless carriers, achieving bit error rates (BERs) below 10^{-5} in the first two cases. The presented experimental demonstration highlights the ability of photomixers to act as transmitters and receivers for sub-THz and THz signals and to enable a huge frequency tuning range for THz communication links.

II. All-Photonics-Based THz Communications

A. Signal generation and detection

The THz wave is generated and detected by the process called photomixing, also known as optical heterodyning if data is transported [22], [23]. For signal generation, a CW THz emitter based on a p-i-n photodiode (PD) is used [24]. If the PD is driven by two optical tones with powers P_1^{TX}, P_2^{TX}, with an angular frequency difference ω_{THz}, and one of them carries data modulation with information in amplitude $s(t)$ and in phase $\phi(t)$, a THz signal is produced with a field (E_{THz}) proportional to:

$$E_{\mathrm{TX}} \propto s(t)\sqrt{P_1^{\mathrm{TX}}P_2^{\mathrm{TX}}}\cos(\omega_{\mathrm{THz}}t+\phi(t)+\phi_{\mathrm{sys,TX}}) \quad (1)$$

where $\phi_{\mathrm{sys,TX}}$ accounts for the phase difference between the two mixed optical tones due to different propagation paths and different initial phases. It is clear that using separate free-running lasers, without phase locking, will greatly impact on the phase noise of the THz signal since $\phi_{\mathrm{sys,TX}}$ will have a strong random time dependence.

On the receiver side, a CW THz receiver based on a PCA is used [24]. Similarly, a beat signal produced by the addition of two optical tones with powers P_1^{RX} and P_2^{RX} biases the receiver antenna, behaving as a local oscillator (LO) whose field is proportional to:

$$E_{\mathrm{LO}} \propto \sqrt{P_1^{\mathrm{RX}}P_2^{\mathrm{RX}}}\cos(\omega_{\mathrm{LO}}t+\phi_{\mathrm{sys,RX}}) \quad (2)$$

where ω_{LO} is the angular frequency difference between the two tones and $\phi_{\mathrm{sys,RX}}$ represents the phase difference. Again, the phase noise of the resulting signal is highly determined by the phase relation between the two optical tones. The LO signal mixes with the received signal after wireless propagation, producing a current at an intermediate frequency (IF), $\omega_{\mathrm{IF}} = |\omega_{\mathrm{THz}} - \omega_{\mathrm{LO}}|$, proportional to:

$$i_{\mathrm{IF}} \propto s(t)\sqrt{P_1^{\mathrm{TX}}P_2^{\mathrm{TX}}P_1^{\mathrm{RX}}P_2^{\mathrm{RX}}}\cos(\omega_{\mathrm{IF}}t+\phi(t)+\phi_{\mathrm{sys,TX}}-\phi_{\mathrm{sys,RX}}) \quad (3)$$

The amplitude and phase components of the modulation, $s(t)$ and $\phi(t)$, can be recovered at the IF after demodulation. Polarization matching between the optical signals used for photomixing is assumed in all cases. The bandwidth of the received signal is limited by the electronics after down-conversion. The receiver module used for this demonstration has an electrostatic discharge protection circuit that behaves as a band-pass filter and limits the usable bandwidth to a 400-MHz window around 3.7 GHz. This device is originally designed for spectroscopy applications in which signals with frequencies in the order of kHz are detected, and not to support IFs above 1 MHz. However, the same devices can be designed without these limitations, so they become suitable for broadband communications [19].

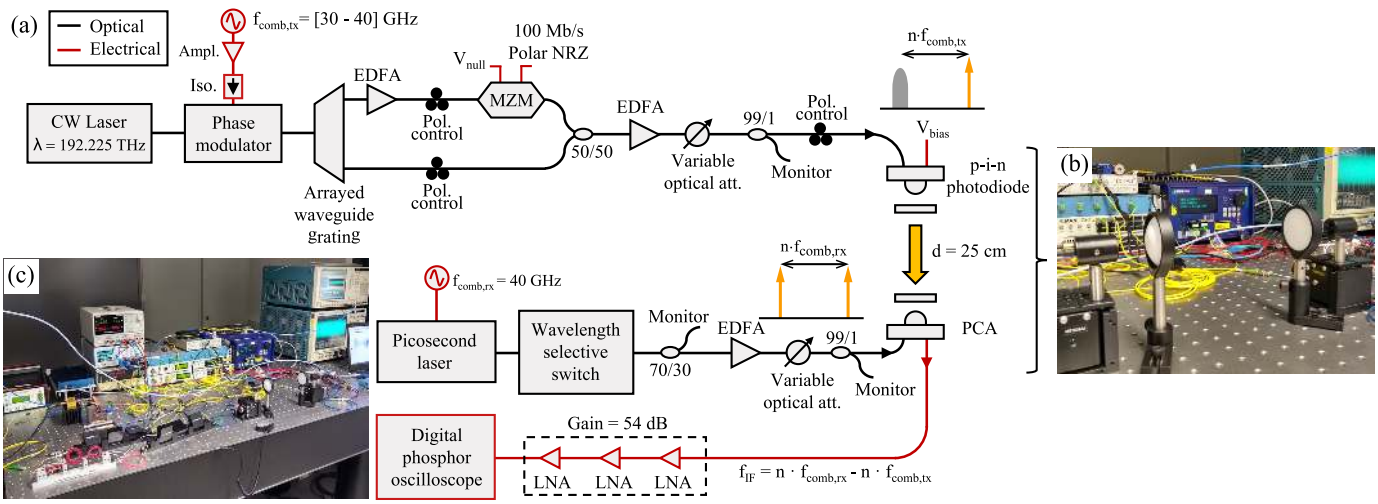

Fig. 2. Experimental setup for the demonstration of a sub-THz communication link using optoelectronic techniques at both ends: (a) block diagram, CW: continuous wave, EDFA: erbium-doped fiber amplifier, MZM: Mach-Zehnder modulator, PCA: photoconductive antenna, LNA: low noise amplifier; (b) photo of wireless link and (c) photo of experiment setup.

B. Optical frequency combs

An OFC is an optical signal whose spectrum consists of a series of equally spaced frequency lines that are phase coherent with one another [25]. It can be defined in the frequency domain according to $f_n = f_0 + nf_\mathrm{r}$, where n is an integer, f_r is the repetition rate and f_0 the frequency offset. One of the many applications of OFCs is the THz signal generation. Two spectral lines with the intended frequency difference can be filtered and used for photomixing, generating a low phase noise signal. There are some parameters that describe a comb which are relevant for THz generation: first, the bandwidth, defined as the total bandwidth occupied by the spectral lines. This bandwidth must be sufficient to achieve the frequency difference of the desired THz signal. Second, the repetition rate, which is related to the optical filters needed to extract the desired lines. If the repetition rate is high, the optical filtering is easier, but the radio frequency (RF) sources and electronics components needed for phase locking are more complex. On the other hand, if the repetition rate is low, the comb source becomes simpler and the optical filtering more challenging. Another important parameter is the tunability of the comb.

There are several ways to generate OFCs [25]. Two different methods are used in this work. Mode-locked lasers (MLLs) are one of the simplest ways to obtain an OFC. MLLs produce very short optical pulses in time (in the order of ps or fs), which correspond to the addition of the different resonant cavity modes. It is possible to generate broadband combs with a relatively high repetition rate using MLLs. However, the tuning range of the repetition rate is small. Another simple approach is using an optical phase modulator to modulate a single laser source with a high-power CW electronic oscillator. The different harmonics produced with the modulation create the comb. The comb bandwidth is limited by the RF power that can be supplied by the electronic source and handled by the modulator. The main advantage of this approach is the tunability of the repetition rate, which is only limited by the operational bandwidth of the modulator.

III. Experimental Setup

Figure 2 shows the experimental setup used to demonstrate a sub-THz communication link based on photonic up-conversion with a p-i-n PD for signal generation and a PCA for heterodyne down-conversion to an IF. Two optical tones, which are extracted from different OFCs, are used as optical inputs in both cases. At the transmitter, the comb is generated by modulating a CW laser source with a phase modulator driven by an external RF source. The signal source produces a sinusoid with frequency $f_{\mathrm{comb,TX}}$, fixing the repetition rate of the comb. This signal is boosted by a power amplifier in order to increase the number of effective harmonics. The operation bandwidth of this amplifier (30 – 40 GHz) sets the tunability range for the repetition rate of this OFC. The electrodes of the phase modulator have been modified to dissipate high RF power, up to 2 W. This scheme results in a comb with a bandwidth above 300 GHz.

Two comb lines are filtered by an 8-channel arrayed waveguide grating (AWG) following the dense wavelength division multiplexing (DWDM) recommendation with a channel spacing of 50 GHz [26]. The 3-dB passband bandwidth of the optical filters is approximately 42 GHz. The frequency of the laser is therefore fixed to 192.225 THz, the center of the AWG bandwidth. The first line is amplified by an erbium-doped fiber amplifier (EDFA) and modulated with a Mach-Zehnder modulator (MZM). The MZM is biased at the null point of its transmission function for two reasons: first, the optical carrier is suppressed, and thus the modulation-to-noise ratio increases after optical-to-electrical conversion. Second, a binary phase-shift keying (BPSK) modulation is produced when launching a 100 Mbit/s polar non-return-to-zero (NRZ) signal into the RF port of the MZM. The data signal is generated by an arbitrary waveform generator using a pseudo-random bit sequence (PRBS) with 2^9-1 bits. The polarization of the second line is controlled by a polarization controller to maximize the generated THz power, and it is recombined with the modulated signal using a 3-dB coupler.

TABLE I
EXPERIMENT PARAMETERS

Wireless Carrier [GHz]	$f_{\mathrm{comb,TX}}$ [GHz]	$f_{\mathrm{comb,RX}}$ [GHz]	n	f_{IF} [GHz]
79.62	37.96	39.81	2	3.70
119.44	38.52	39.81	3	3.88
159.25	38.88	39.81	4	3.74
199.07	39.07	39.81	5	3.71
238.89	39.19	39.81	6	3.72
278.69	39.27	39.81	7	3.78
318.51	39.35	39.81	8	3.70

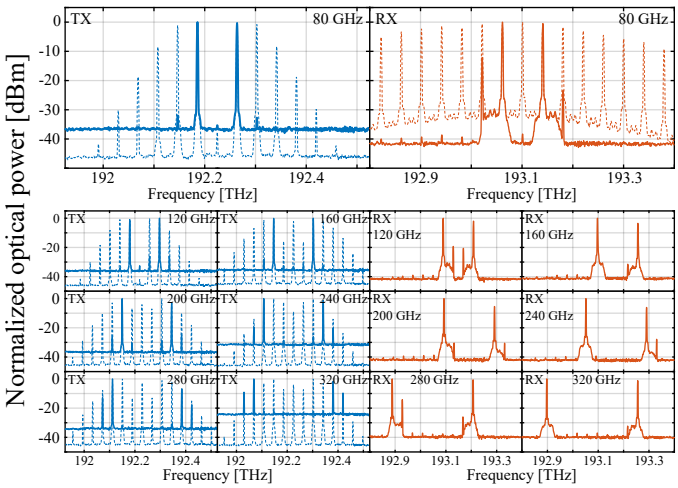

Fig. 3. Normalized spectra of OFCs (dashed lines) and optical signals after filtering for photomixing (solid lines).

After the combiner, the signal is amplified by a second EDFA to set the maximum optical power incident on the photodiode to 30 mW (15 dBm). A variable optical attenuator (VOA) and a 99%/1% coupler control the optical power for BER measurements. This signal is converted into the THz domain by a THz emitter based on a p-i-n diode, and it is radiated by a THz antenna attached to the diode contacts and a silicon lens. A couple of Teflon lenses are also added to further collimate the THz beam across a 25 cm wireless link.

At the receiver, a MLL is used as the comb source. The repetition rate can be fixed within a small fine-tuning range around $f_{\mathrm{comb,RX}} = 40$ GHz, using an external LO. A wavelength selective switch (WSS), also following the 50-GHz DWDM grid [26], is used to extract the two comb lines used to bias the photoconductor on a single fiber. The 3-dB passband bandwidth of the optical filters is approximately 35 GHz. An EDFA, a VOA and a 99%/1% coupler are used again to set and control the optimum optical power required by the photoconductor to bias the receiver THz antenna and detect the transmitted wave. This optical power is fixed to 30 mW (15 dBm). As a result, the recovered signal is down-converted to an IF and amplified by three cascaded low noise amplifiers LNAs with an overall gain of 54 dB and an operating bandwidth of 6 GHz. The signal is finally captured by a digital phosphor oscilloscope (DPO) for off-line processing. The experiment was conducted inside a Faraday cage to avoid external RF interference.

The major benefit of this scheme is its wide tunability. The wireless carrier can be selected by tuning $f_{\mathrm{comb,TX}}$ and filtering the proper optical lines. The main limitation is imposed by the bandwidth of the RF amplifier and the fact that the filter bandwidth is higher than the repetition rate of the comb. Seven wireless channels with 40 GHz difference (from 80 GHz to 320 GHz) are tested. Table I lists the parameters used in the transmitter to establish these channels and Fig. 3 shows the optical spectra of the filtered signal (solid line), compared with the input comb (dashed line). There are some important points about these graphs to be noted. The amplitude of the different harmonics in the input comb is strongly related to the RF power [27]. This feature can also be used to improve the filtering by decreasing the power of unwanted harmonics. The mismatch between the filter bandwidth and the comb period becomes more significant as higher-order harmonics are used. For instance, an important part of the neighbouring lines is also passed by the filter in the 280 GHz and 320 GHz cases. The power of these harmonics is also lower due to the comb shape. Since an EDFA operating in automatic power control mode is used to provide constant optical power to the PD, this fact is translated into an apparent increase in the noise floor.

In a similar way, the wireless signal to be detected can be selected by filtering the proper comb lines driving the photoreceiver. The repetition rate, $f_{\mathrm{comb,RX}}$, is in this case fine-tuned around 40 GHz. The intermediate frequency is therefore given by the difference in the repetition rate between the two OFCs according to $f_{\mathrm{IF}} = nf_{\mathrm{comb,RX}} - nf_{\mathrm{comb,TX}}$, where f_{IF} is the IF and n is an integer. As explained in the previous section, f_{IF} can be tuned around 3.7 GHz with a modulation bandwidth up to 400 MHz. The receiver parameters are listed in Tab. I and the optical spectra are also shown in Fig. 3. In this case, the shape of the comb does not change, although the center frequency was slightly tuned. There is again a mismatch between the repetition rate of the comb and the bandwidth of the filters, so part of unwanted comb lines passes through. This effect is particularly noticeable in the 80 GHz, 120 GHz, and 240 GHz cases. However, the additional tones are maintained sufficiently attenuated compared to the main lines, more than 10 dB in the worst case and more than 20 dB in most configurations. These values allow the wireless signal to be downconverted to the intended intermediate frequency.

IV. RESULTS AND DISCUSSION

A. System spectrum

The first test was the validation of the heterodyne THz system transmitting a pure tone without data. The power of the received signal, after amplification, was measured with a 40-GHz-bandwidth electrical spectrum analyzer (ESA), obtaining the IF peak powers plotted in Fig. 4. These results prove a system bandwidth of more than 240 GHz and a maximum signal-to-noise ratio of approximately 39.7 dB at 80 GHz. The main limitation comes from the transmitter OFC bandwidth and the noise of the LNAs used after the photoconductor. Although they have a relatively low noise figure of 3.8 dB, it is high compared with transimpedance amplifiers used in traditional spectroscopy systems, which require much smaller

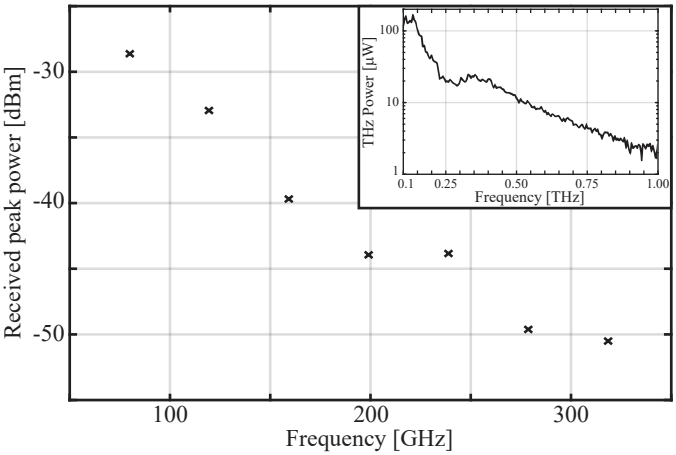

Fig. 4. Received peak power without modulation versus frequency compared with transmitted THz transmitter power according to datasheet.

bandwidths. The distribution of the points agrees with the generated THz power in the emitter (inset of Fig. 4), although more factors contribute to these results. The sensitivity of the photoconductor is also frequency-dependent, and the optical signals launched into emitter and receiver are not pure tunes and not equal for each wireless carrier (see Fig. 3). The wireless propagation loss also varies with the frequency. This additional attenuation is partly overcome by the Teflon lenses that increase the effective antenna gain.

B. Phase Noise

An important parameter that largely determines the performance of the data link is the phase noise. As shown by Eqs. 1 – 3, the use of phase-locked optical signals for photomixing significantly reduces the phase noise of the THz waves, enabling the transmission of complex phase modulation schemes. The phase noise measurement functionality of the 40-GHz-bandwidth ESA was used to measure the phase noise at different points in the transmitter and receiver systems.

The phase noise measurements at the transmitter branch are depicted in Fig. 5(a). The curve that represents the phase noise of the RF source has a relatively flat response of 100 dBc/Hz in the 1 – 30 kHz range with the characteristic $1/f^2$ negative slope beyond 30 kHz. This electrical signal has a significant impact on the phase of the transmitter side. The full comb is used as the input to a 40-GHz PD to analyze the beating product at $f_{\mathrm{comb,TX}}$. Although the shape of the curve follows the behavior of the electrical source in the low frequencies, the power of the signal is very low. This is due to the phase relation between symmetric harmonics of the comb, which causes destructive interference. If the same measurement is repeated after filtering the center carrier and half of the comb, a curve that closely follows the original RF source is obtained. The filtering was done, in this test, with the WSS because it allowed the extraction of the intended comb lines without using separate fibers and combiners.

Figure 5(a) also plots the phase noise at the output of the 50%/50% combiner, after filtering with the AWG and following the arrangement in Fig. 2. Two consecutive tones (beating

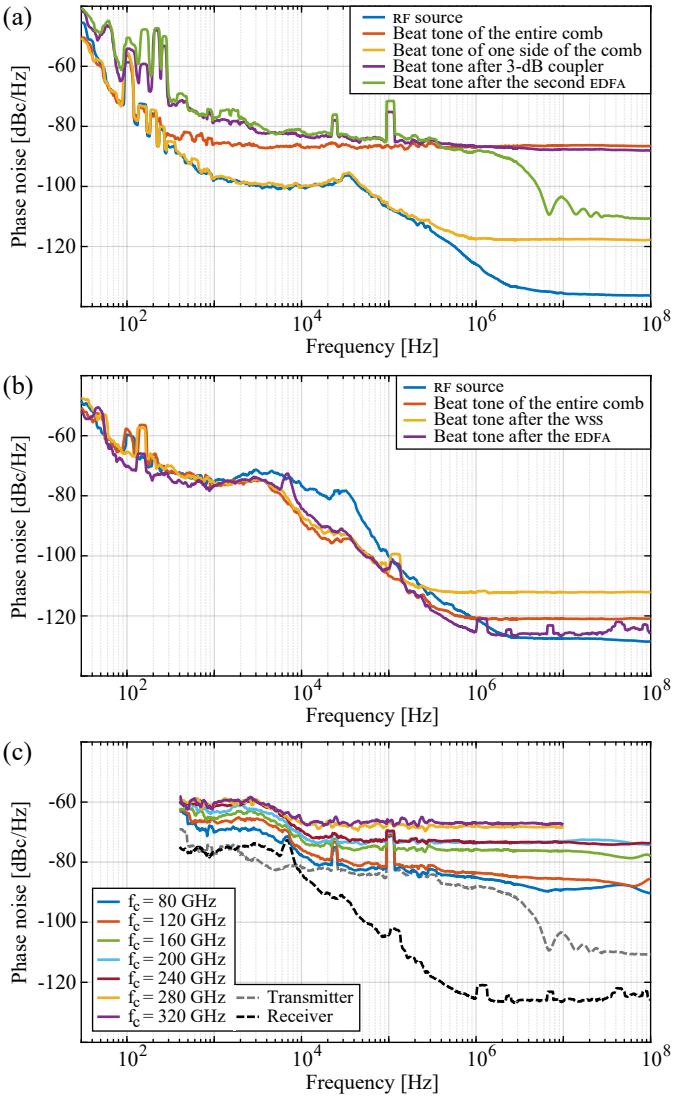

Fig. 5. Phase noise measurements at: (a) different points in the transmitter system, (b) different points in the receiver system and (c) received signal at intermediate frequency after sub-THz wireless transmission.

product at $f_{\mathrm{comb,TX}}$) are used for this measurement, due to the bandwidth limitation of the ESA. The power of the signal at this point is low, but an increment in the phase noise level is observed. This increase appears because the two optical components used for photomixing propagate through separate optical fibers with different lengths [28]. Two additional peaks appear at 24 kHz and 100 kHz, which are attributed to the filtering and the control loop of the EDFA in one of the two lines. Finally, the phase noise measurement after the second EDFA matches with the previous one, with a small increment, for frequencies below 1 MHz. For frequencies above 1 MHz, an oscillation with a slope steeper than $1/f^2$ appears. This behavior has already been studied, and it is produced due to the interferometer formed by the arrangement of the system [29]. These results show that the phase noise behavior of the produced signal is largely determined by the length unbalance between the two arms of the system and the electrical source [28], [29].

The same analysis is done for the receiver, as shown in Fig. 5(b). The phase noise characteristic of the reference RF source is worse than the one used for the transmitter. It has an approximately flat response above −80 dBc/Hz in the 0.3 – 20 kHz range and the $1/f^2$ negative slope starting at 30 kHz. A noise reduction is observed at frequencies above 2 kHz in the curve corresponding to the beat tone of the entire comb. This reduction is attributed to the internal electronic circuit for phase-locking. The same behavior was not observed when better signal sources were used. Again, the phase noise of the comb beating is mainly determined by the RF source. The problem related to the phase difference between lines does not appear in this case because each line corresponds to different cavity modes. A reduction in the power and the apparition of a peak at 120 kHz are recognizable after filtering two tones with the WSS. This demultiplexer allows the extraction of the two optical components to the same optical fiber, so the increment in phase noise observed in the transmitter system does not appear in the receiver. Finally, a new peak appears at 7 kHz due to the last EDFA. The final phase noise curve is essentially determined by the electronic source, as expected.

The phase noise behavior after the wireless transmission and down-conversion is clearly the superposition of the phase noise curves at the transmitter and receiver, with the same characteristic peaks appearing in the recovered signals: 24 kHz, 100 kHz and 120 kHz. The phase noise contribution of the transmitter is more relevant at high frequencies, while the contribution of the receiver is dominant at lower frequencies. The power of the receiver signal is low, making the $1/f^2$ negative slope impossible to distinguish. The detected power decreases with frequency with the same relation discussed in Fig. 4. It can be drawn from these results that the phase noise is mainly determined by the electronics used for optical phase locking, the fiber length unbalance in the transmitter side, and the signal power.

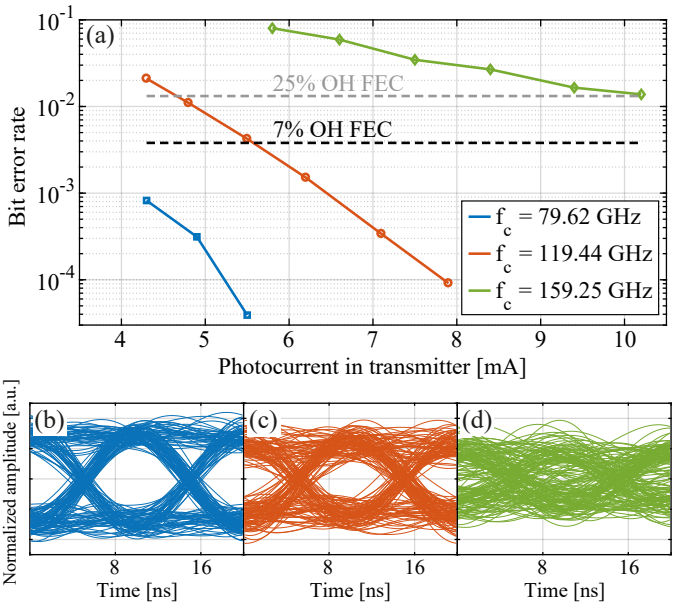

Fig. 6. Data transmission results: (a) bit error rate curves versus photocurrent generated in the transmitter and eye diagrams after demodulation when the transmitted power was 10.2 mA and the wireless carrier was (b) 79.62 GHz, (c) 119.44 GHz and (d) 159.25 GHz.

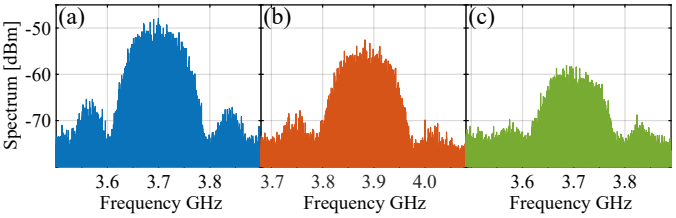

Fig. 7. Electrical Spectra of the received signal when the transmitted power was 10.2 mA and the wireless carrier was (a) 79.62 GHz, (b) 119.44 GHz and (c) 159.25 GHz.

C. Data Transmission

The last experiment was the data transmission of a 100 Mbit/s BPSK stream over different wireless channels with 40 GHz spacing. The BER measurements for 79.62 GHz, 119.44 GHz and 159.25 GHz carriers compared with the photocurrent generated by the PD are shown in Fig. 6(a). The traces captured with the DPO were digitally demodulated using digital filters and a Costas loop algorithm for carrier recovery, without further equalization. The maximum photocurrent $I_{\mathrm{ph,MAX}} = 10.2\,\mathrm{mA}$ corresponds to the optimum value for the optical power, which is 30 mW (15 dBm) and produces the wireless signal power displayed in Fig. 4. For this value, the BER is below 10^{-5} when transmitting over the 79.62 GHz and 119.44 GHz channels and it increases to the limit of forward error correction (FEC) techniques with 25 % overhead when the carrier is 159.25 GHz. The data could not be recovered for higher frequencies due to a lack of received signal power.

The 79.62 GHz BER curve is maintained below 10^{-5} until the photocurrent is decreased to 5.4 mA, and below the FEC limit with 7 % overhead over the full measurement range. The eye diagram for the maximum photocurrent is shown in Fig. 6(b). The 119.44 GHz BER increases due to the lower SNR. However, it is below the limit for a FEC with 7 % overhead when the emitter photocurrent is more than 5.6 mA. The eye diagram depicted in Fig. 6(c) is worse compared with the previous one, but stays open. The last curve, corresponding to 159.25 GHz, represents a great increase in the BER as it can also be seen in the closed eye diagram in Fig. 6(d). The BER increase at 159.25 GHz is noticeable compared to the previous curves. This may be caused by the worse response of the signal processing algorithms when the signal power is low.

The BER performance of the link is primarily determined by the link SNR. The optical fiber length is too short to observe significant chromatic dispersion, and the wireless link is very directive, so no multipath effects appear. This can also be seen in the symmetry of eye diagrams in Figs. 6(b)-(d) and in the shape of the received electrical spectra in Fig. 7. The SNR decreases as the wireless carrier increases without any significant deformation in the signal spectrum. This means that the curves in Fig. 6(a) can be prolonged if the transmitted SNR is increased. More efficient CW THz emitters and antenna arrays combining several sources are two possible solutions to enhance the system bandwidth.

V. Conclusion

A full-photonic heterodyne sub-THz system was demonstrated, detecting wireless waves transmitted at seven different carriers, ranging from 80 GHz to 320 GHz in 40 GHz steps, with an intermediate frequency of 3.7 GHz. The power variation was higher than 21.8 dB over a 240 GHz frequency span. Independent optical sources were employed for photomixing at both ends of the communication link. Optical frequency combs were used to reduce the phase noise of the resulted sub-THz signals to increase the dynamic range of the system and improving the performance when phase modulated signals are transmitted. The OFCs were generated with an external phase modulator and a mode-locked laser. The phase noise of the transmitter, receiver, and recovered signals was analyzed, concluding that it is mainly determined by the RF sources needed for optical comb generation and the fiber length unbalance between the two arms in the transmitter system. Finally, a 100 Mb/s BPSK data stream was successfully transmitted over 79.62 GHz, 119.44 GHz and 159.25 GHz wireless carriers, achieving a BER below 10^{-5} in the first two cases. This performance was limited by the SNR, and thereby the presented results of frequency range and BER can be improved by using more efficient signal sources, optimized for operation in the lower region of the THz spectrum, and antenna arrays.

This work represents an important step towards the full exploitation of the sub-THz and THz ranges for ultra-broadband short-range wireless communications. The optical domain offers a wide range of possibilities to THz communications through optoelectronic techniques for signal generation and detection. However, power amplifiers and other electronic components, which are, in most cases, required to overcome the high propagation loss, limit the frequency tuning range. Technical advances in photonic integration and THz sources and detectors offer a great potential to integrate on-chip complex systems like the one described in this work. THz links entirely relying on photonics represent one of the leading candidates to implement highly tunable, ultra-broadband, multi-channel, and bidirectional THz communications in the future.

References

[1] T. Nagatsuma, G. Ducournau, and C. C. Renaud, "Advances in terahertz communications accelerated by photonics," *Nat. Photonics*, vol. 10, no. 6, pp. 371-379, Jun. 2016, doi: 10.1038/nphoton.2016.65.

[2] T. Schneider, "Ultrahigh-Bitrate Wireless Data Communications via THz-Links; Possibilities and Challenges," *J. Infrared Millim. Terahertz Waves*, vol. 36, no. 2, pp. 159-179, Feb. 2015, doi: 10.1007/s10762-014-0100-1.

[3] A. J. Seeds, H. Shams, M. J. Fice, and C. C. Renaud. "Terahertz photonics for wireless communications," *J. Light. Technol.*, vol. 33, no. 3, pp. 579-587, Sep. 2014, doi: 10.1109/JLT.2014.2355137.

[4] M. Tonouchi, "Cutting-edge terahertz technology," *Nat. Photonics*, vol. 1, no. 2, pp. 97-105, Feb. 2007, doi: 10.1038/nphoton.2007.3.

[5] D. Hou, J. Chen, P. Yan, and W. Hong, "A 270 GHz x 9 multiplier chain MMIC with on-chip dielectric-resonator antenna," *IEEE Trans. Terahertz Sci. Technol.*, vo. 8, no. 2, pp. 224-230, Jan. 2018, doi: 10.1109/TTHZ.2017.2786027.

[6] K. M. K. H. Leong, *et al.*, "850 GHz receiver and transmitter front-ends using InP HEMT," *IEEE Trans. Terahertz Sci. Technol.*, vo. 7, no. 4, pp. 466-475, Jun. 2017, doi: 10.1109/TTHZ.2017.2710632.

[7] S. Diebold, *et al.*, "High-speed error-free wireless data transmission using a terahertz resonant tunnelling diode transmitter and receiver," *Electronics Letters*, vol. 52, no. 24, pp. 1999-2001, Nov. 2016, doi: 10.1049/el.2016.2941.

[8] A. Morales, R. Puerta, S. Rommel, and I. Tafur Monroy, "1 Gb/s chaotic encoded W-band wireless transmission for physical layer data confidentiality in radio-over-fiber systems," *Opt. Express*, vol. 26, no. 17, pp. 22296-22306, Aug. 2018, doi: 10.1364/OE.26.022296.

[9] M. Urteaga, Z. Griffith, M. Seo, J. Hacker, and M. J. W. Rodwell, "InP HBT Technologies for THz Integrated Circuits," *Proc. IEEE*, vol. 105, no. 6, pp. 1051-1067, May 2017, doi: 10.1109/JPROC.2017.2692178.

[10] K. M. K. H. Leong, *et al.*, "A 0.85 THz Low Noise Amplifier Using InP HEMT Transistors," *IEEE Microw. Wirel. Compon. Lett.*, vol. 25, no. 6, pp. 397-399, Apr. 2015, doi: 10.1109/LMWC.2015.2421336.

[11] V. K. Chinni, *et al.*, "Single-channel 100 Gbit/s transmission using III–V UTC-PDs for future IEEE 802.15. 3d wireless links in the 300 GHz band," *Electron. Lett.*, vol. 54, no. 10, pp. 638-640, May 2018, doi: doi: 10.1049/el.2018.0905.

[12] C. Castro, *et al.*, "32 GBd 16QAM wireless transmission in the 300 GHz Band using a PIN Diode for THz upconversion," in *Proc. Opt. Fiber Commun. Conf. Exhib. (OFC)*, pp. M4F.5, Mar. 2019, doi: 10.1364/OFC.2019.M4F.5.

[13] H. Shams, *et al.*, "Photonic generation for multichannel THz wireless communication," *Opt. Express*, vol. 22, no. 19, pp. 23465–23472, Sep. 2014, doi: 10.1364/OE.22.023465.

[14] A. d. J. Fernandez Olvera, H. Lu, A. C. Gossard, and S. Preu "Continuous-wave 1550 nm operated terahertz system using ErAs: In (Al) GaAs photo-conductors with 52 dB dynamic range at 1 THz," *Opt. Express*, vol. 25, no. 23, pp. 29492-29500, Nov.. 2017, doi: 10.1364/OE.25.029492.

[15] International telecommunication union, "Recommendation ITU-R P.676-12: Attenuation by atmospheric gases and related effects", *P Series Radiowave Propagation*, Aug. 2019.

[16] A. Morales, *et al.*, "Bidirectional K-band photonic/wireless link for 5G communications." In *44th International Conference on Infrared, Millimeter, and Terahertz Waves (IRMMW-THz)*, pp. 1-2, Sep. 2019, doi: 10.1109/IRMMW-THz.2019.8874031.

[17] A. Morales, *et al.*, "Photonic-Based Beamforming System for Sub-THz Wireless Communications", in *European Microwave Conference in Central Europe (EuMCE)*, pp. 253–256, May 2019.

[18] S. Rommel, T. R. Raddo, and I. Tafur Monroy, "Data Center Connectivity by 6G Wireless Systems," in *Photonics in Switching and Computing*, Fr3B.1, Sep. 2018, doi: PS.2018.8751363.

[19] Y. Dong, *et al.*, "System integration and packaging of a terahertz photodetector at W-band," *IEEE Trans. Compon. Packag. Manuf. Technol.*, vol. 9, no. 8, pp. 1486–1494, Jul. 2019, doi: 10.1109/TCPMT.2019.2928053.

[20] T. Harter, *et al.*, "Wireless Multi-Subcarrier THz Communications Using Mixing in a Photonconductor for Coherent Reception," in *Proc. IEEE Photonics Conf. (IPC)*, pp. 147–148, Oct. 2017, doi: 10.1109/IPCon.2017.8116044.

[21] T. Harter, *et al.*, "Wireless THz link with optoelectronic transmitter and receiver," *Optica*, vol. 6, no. 8, pp. 1063–1070, Aug. 2019, doi: 10.1364/OPTICA.6.001063.

[22] S. Preu, G. H. Döhler, S. Malzer, L. J. Wang, and A. C. Gossard, "Tunable, continuous-wave terahertz photomixer sources and applications," *J. Appl. Phys*, vol. 109, no. 6, pp. 4, Mar. 2011, doi: 10.1063/1.3552291.

[23] J. Yao, "Microwave photonics" *J. Light. Technol.* vol. 27, no. 3, pp. 314–335, Feb. 2009, doi: 10.1109/JLT.2008.2009551.

[24] S. Nellen, B. Globisch, R. B. Kohlhaas, L. Liebermeister, and M. Schell, "Recent progress of continuous-wave terahertz systems for spectroscopy, non-destructive testing, and telecommunication," In *THz, RF, MM, and Submm-Wave Tech. and Appl. XI*, vol. 10531, p. 105310C, Feb. 2018, doi: 10.1117/12.2290207.

[25] T. Fortier and E. Baumann. "20 years of developments in optical frequency comb technology and applications," *Commun. Phys.*, vol. 2, no. 1, pp. 1–16, Dec. 2019, doi: 10.1038/s42005-019-0249-y.

[26] International telecommunication union, "Recommendation ITU-T G.694.1: Spectral grids for WDM applications: DWDM frequency grid," *G Series: Transmission systems and media, digital systems and networks*, Feb. 2012.

[27] G. Qi, J. Yao, J. Seregelyi, S. Paquet, and C. Bélisle, "Optical generation and distribution of continuously tunable millimeter-wave signals using an optical phase modulator," *J. Light. Technol.*, vol. 23, no. 9, pp. 2687–2695, Sep. 2005, doi: 10.1109/JLT.2005.854067.

[28] J. Pérez Santacruz, S. Rommel, U. Johanssen, A. Jurado-Navas, and I. Tafur Monroy, "Analysis and Compensation of Phase Noise in mm-Wave OFDM ARoF Systems for Beyond 5G," *J. Light. Technol.*, Nov. 2020, doi: 10.1109/JLT.2020.3041041.

[29] T. Shao, F. Paresys, G. Maury, Y. Le Guennec, and B. Cabon, "Investigation on the phase noise and EVM of digitally modulated millimeter wave signal in WDM optical heterodyning system," *J. Light. Technol.* vol. 30, no. 6, pp. 876–885, Jan. 2012, doi: 10.1109/JLT.2012.2183340.

Alvaro Morales (S'18) was born in León, Spain, in 1992. He received the B.Sc. degree in telecommunication technologies engineering and the M.Sc. degree in telecommunications engineering from the University of Valladolid (UVa), Spain, in 2014 and 2016, respectively. He worked as a student assistant at the Photonics Engineering Department, Technical University of Denmark (DTU) between 2015 and 2017.

He is currently pursuing the Ph.D. degree at the Technical University of Eindhoven (TU/e), Netherlands, under the framework of the EU H2020 project CELTA. His research interests include millimeter-wave and sub-terahertz communications, radio-over-fiber systems, beamforming and photonic integration.

Gleb Nazarikov received his B.Sc. degree in Physics from Novosibirsk State University (NSU), Russia, in 2017 and M.Sc. degree in Photonics in 2019 from Skolkovo Institute of Science and Technology (Skoltech), Moscow, Russia. He is currently PhD student at Technical University of Eindhoven (TU/e), Netherlands. His research field of interests include analog radio-over-fiber systems, fiber communications and photonic integration.

Simon Rommel (S'15–M'18) obtained his B.Sc. degree from the University of Stuttgart, Germany in 2011 and in 2014 obtained M.Sc. degrees in Photonic Networks Engineering from Aston University, Birmingham, UK and Scuola Superiore Sant'Anna, Pisa, Italy. He completed his Ph.D. in 2017 at the Technical University of Denmark, Kongens Lyngby, Denmark with research focused on photonic-wireless convergence and millimeter-wave radio-over-fiber links. In 2017 he visited the National Institute of Information and Communications Technology, Koganei, Tokyo, Japan for a research stay.

Since 2017 he is with Eindhoven University of Technology, currently as an assistant professor, continuing his work photonic and radio frequency technologies with a strong focus on implementations for 5G. His research interests include the fields of fiber-optic and wireless communications and the associated digital signal processing. He has contributed to multiple national and European research projects, incl. H2020 blueSPACE as technical manager.

Dr. Rommel is a member of Institute of Electrical and Electronics Engineers (IEEE), The Optical Society (OSA), the Institution of Engineering and Technology (IET) and the Verband der Elektrotechnik Elektronik Informationstechnik e.V (VDE).

Chigo Okonkwo (M'09–SM'18) was born in Wakefield, U.K., in 1979. He received the Ph.D. degree in optical signal processing from the University of Essex, Colchester, U.K., in 2010. Between 2003 and 2009, he was a Senior Researcher with the Photonic Networks Research Lab, University of Essex, U.K. After his Ph.D., he was appointed as a Senior Researcher with the Electro-optical communications group working on digital signal processing techniques and the development of space division multiplexed transmission (SDM) systems.

As an associate professor, he currently leads the High-capacity optical transmission laboratory within the Institute for Photonic Integration (former COBRA), Department of Electrical Engineering, Eindhoven University of Technology (TU/e),The Netherlands. He was instrumental to the delivery of the first major SDM project in the European Union—MODEGAP project. Since 2014, he has been tenured at the ECO group, where he has since built up a world-class laboratory collaborating with several industrial and academic partners. His general research interests are in the areas of 5G radio, optical and digital signal processing, space division multiplexing techniques, and long-haul transmission techniques. In 2018, he was TPC chair for subcommittee 3 on digital signal handling. Between 2015 and 2017, he served on the TPC for the OSA conference on signal processing in photonic communications (SPPCom). In 2017 and 2018, he was the Program Chair and the Conference Chair at SPPCom, respectively. Dr. Okonkwo recently served as an associate editor for special edition of the IEEE Journal on Lightwave Technology. For the next 3 years, he has been elected to serve as technical programme subcommittee on fiber-optic and waveguide devices and sensors (subcommittee D5) at Optical fiber communications conference OFC 2020.

Idelfonso Tafur Monroy is since July 2017, Professor in photonic Terahertz systems at the department of Electrical Engineering of the Eindhoven University of Technology, and since November 2018 director of the Photonic Integration Technology Center (PITC).

He coordinates the 5G PPP BLUESPACE project on technologies for 5G wireless systems and the ITN CELTA project with 15 PhD students working convergence of electronics and photonics technologies for applications such as THz communications, sensing and imaging.

His research interests are in the area photonics technologies for Terahertz systems, converged electronic-photonic integrated circuits for applications in secure communications, sensing and computing. He is co-author of over 500 journal and conference papers and has graduated 22 PhD students. He is co-founder of the start-up Bifrost Communications on optical fiber access solutions.

Idelfonso Tafur started his academic career in the Kharkov Polytechnic Institute in Ukraine, he received a M.Sc degree from the Bonch-Bruevitch Institute of Communications, St. Petersburg, Russia, holds a Technology Licentiate degree in telecommunications theory from the Royal Institute of Technology, Stockholm, Sweden, and a PhD degree from the Eindhoven University of Technology.

He has been Professor in photonics communication technologies at Technical University of Denmark, guest Professor at the Beijing University of Post and Telecommunications, visiting scientist at the University of California at Berkeley and Fellowship Professor at the ITMO University in St Petersburg Russia, and is a senior member of IEEE.